

Edge Transport Barrier Formation and Power Threshold Properties in CHS

T. Akiyama¹, S. Okamura¹, T. Minami¹, A. Fujisawa¹, T. Oishi², M. Isobe¹, K. Matsuoka¹, S. Nishimura¹, C. Suzuki¹, K. Nagaoka¹, Y. Yoshimura¹, C. Takahashi¹, M. Yoshinuma¹, S. Kado², H. Iguchi¹, K. Nakamura¹, K. Toi¹, M. Takeuchi³, A. Shimizu¹, K. Ida¹, K. Kawahata¹, S. Tsuji-Iio⁴, S. Okajima⁵, CHS experimental group¹

¹ National Institute for Fusion Science, Toki 509-5292, Japan

² The University of Tokyo, Tokyo 113-8656, Japan

³ Nagoya University, Nagoya 464-8603, Japan

⁴ Tokyo Institute of Technology, Tokyo 152-8550, Japan

⁵ Chubu University, Kasugai, 487-8501, Japan

1. Introduction

The confinement improvement by the formation of edge transport barrier (ETB) is observed in the Compact Helical System (CHS) by inducing large net plasma current [1] and increasing co-injected neutral beam power [2, 3]. Similarly to H-mode in tokamaks, the power threshold exists and depends on various parameters. In this paper we present features of plasma with ETB and the parameter dependences of the power threshold. We also show comparisons with tokamak H-mode power scaling.

2. Features of plasma with ETB in CHS

CHS is a low-aspect-ratio helical device (major radius $R=1.0$ m, minor radius $a=0.2$ m). Figure 1 shows one example of time evolutions of characteristic parameters in a plasma with ETB. In this discharge the magnetic field B is 0.95 T at magnetic axis and the total NB port-through power is 1.4 MW. Following NB injections, spontaneous and sharp drop in $H\alpha$ emission signal is observed. It drops in two steps as illustrated with red arrows. The first drop takes more than several milliseconds, which is comparable to or longer than the energy confinement time. The second takes less than 1 ms. We presume that changes during the first drop

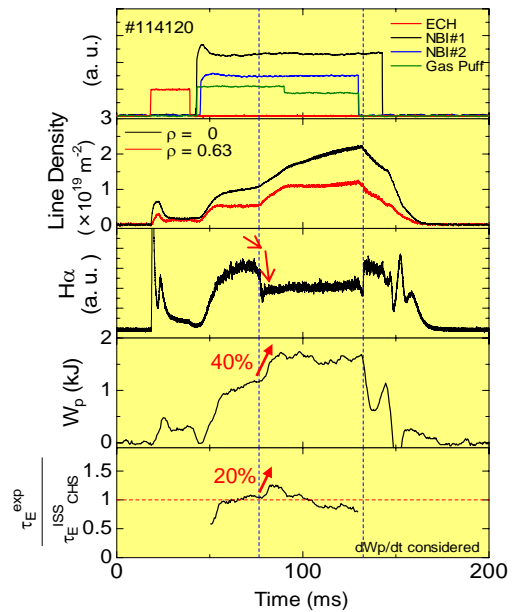


Fig.1: Time evolutions of characteristic parameters in ETB formed plasma. A transition and a back transition occur at $t = 76.5$ and 132.4 ms, respectively.

induce the transition. Line densities especially along plasma edge chord of HCN laser interferometer start to increase simultaneously with the second drop in H α signal. The electron density gradient near the plasma edge becomes steeper after a transition as shown in Fig. 2. These phenomena indicate improvement in edge particle transport. On the contrary the electron and ion temperature profiles do not change. These are different points from H-mode in tokamaks because simultaneous changes in n_e , T_e and T_i profiles have been reported. The

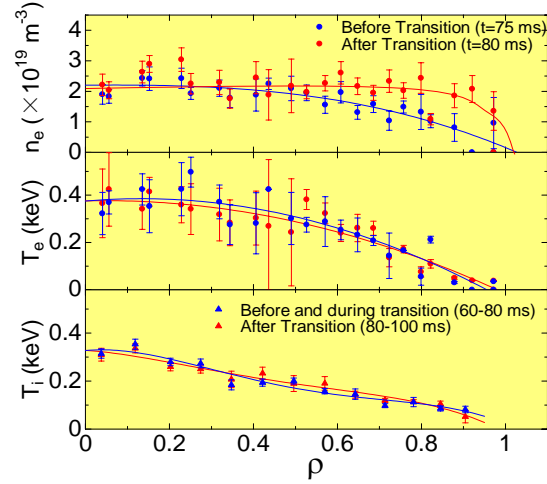


Fig.2: Change in radial profiles before and after transition. n_e and T_e profiles are obtained with a Thomson scattering measurement and T_i profile from charge exchange spectroscopy.

transitions occur with delay times in the range between 5 and 80 ms after NB injections. The delay time depends on the injection power and magnetic configurations. After a transition the stored energy increases by about 40%. In order to evaluate a confinement improvement factor, we use the international stellarator scaling (ISS) 04v3 as given follows [4];

$$\tau_{E\text{CHS}}^{\text{ISS04v3}} = \tau_E^{\text{ISS04v3}} f_{\text{ren}} = 0.0636 a^{2.33} R^{0.64} P_{\text{abs}}^{-0.61} \bar{n}_e^{-0.55} B^{0.85} t_{2/3}^{0.41}$$

where P_{abs} , n_e , $t_{2/3}$ and f_{ren} are absorbed power (in MW), line averaged density (in 10^{20} m^{-3}), rotational transform at ρ of 2/3 and renormalization factor, respectively. f_{ren} is a factor which depends on the magnetic configuration and is 0.43 for CHS. In this analysis the absorbed power is calculated on the basis of the results of Monte Carlo simulation HELIOS code [5]. Based on the ISS04 scaling, the energy confinement is improved by about 20%. The improved state, however, is kept for only about 5 ms and degrades gradually although H α signal keeps at a low level. We infer that this degradation is not related to ETB itself since such degradation is observed in a plasma without ETB.

3. Power threshold and parameter dependence

From NB power-scan experiments the power threshold for transition was found. The NB power approaching to the threshold, the delay time and the first H α drop phase become longer. Spiky H α signals, whose time width is 1-2 ms, are observed when the power is close to the threshold. Finally the second sharp drop in H α signal disappears (“Obscure Transition” shown in Fig. 3) and then the first slow drop does not occur (“No Transition” in Fig. 3).

Dependences of threshold power on plasma and configuration parameters have been studied well and reported in tokamak devices. Figure 3(a) shows the dependence on electron

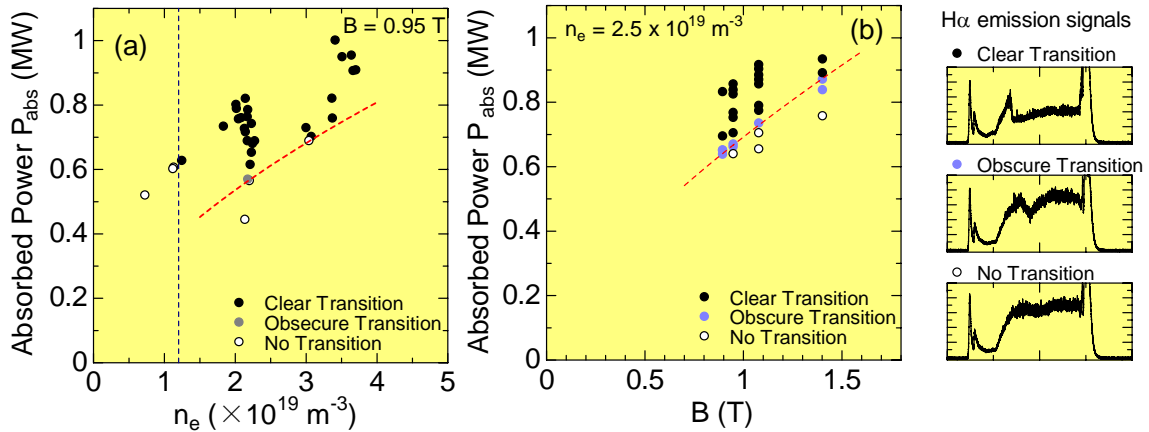


Fig.3 : Dependence of power threshold on (a) line averaged electron density and (b) magnetic field. Black, gray solid circles and open circles denote clear, obscure, no transition, respectively, as shown in right side figures.

density in CHS. In this figure the line averaged electron density at 15 ms after NB injection, that is almost the same as the time of a transition, is plotted. The threshold increases with increasing electron density. In addition the drop in $H\alpha$ signal was not observed for the electron density of less than about $1 \times 10^{19} \text{ m}^{-3}$. The threshold also increases with increasing magnetic field strength as shown in Fig. 3(b). In this magnetic-field-scan experiment electron density at the transition is constant to be $2.5 \times 10^{19} \text{ m}^{-3}$. Although these dependences are similar to those in tokamaks, it is under study whether these similarities are attributed to the same mechanism of ETB formation or not. Furthermore the threshold depends on the magnetic field configurations such as the position of the magnetic axis [6]. The magnetic axis is usually between R of 0.899 and 1.02 m in CHS. The position of magnetic axis where a transition is observed is between R of 0.899 and 0.949 m. In this range the last closed flux surface (LCFS) is determined by the inboard side of vacuum vessel wall and transitions are observed only in the limiter configurations so far. From Fig. 4, it can be seen that the threshold becomes lower in outer shifted configurations. Since electron densities at transitions are not constant in this data set, the absorbed power normalized by electron density is used. Here the dependence on density is considered to be linear approximately because the quantitative estimation is not enough at this moment. This result indicates that there are hidden parameters which are associated with magnetic configuration such as ι at the LCFS, magnetic shear and so on. The magnetic shear near plasma edge region becomes stronger when magnetic axis is shifted to the outward direction in CHS. Strong magnetic shear may help ETB formation. A decisive parameter, however, has not been identified yet.

Figure 5 shows comparison with the threshold predicted from H-mode threshold power scaling derived from divertor tokamaks shown as follows [7];

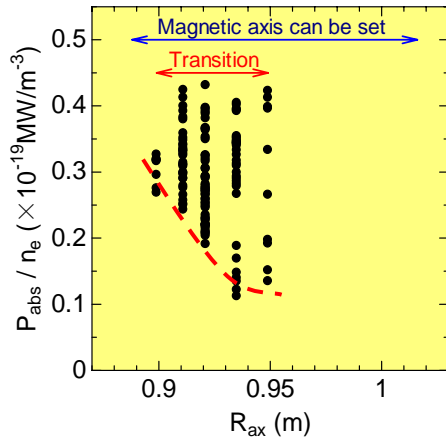


Fig. 4: Dependence of power threshold on the position of magnetic axis.

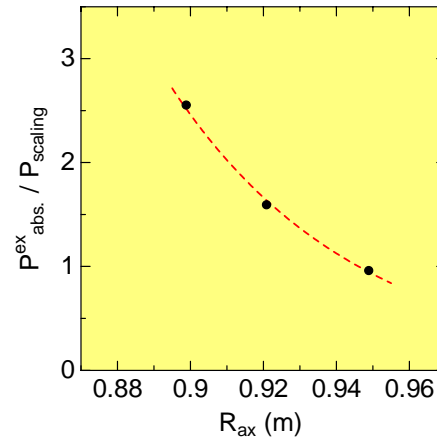


Fig. 5: Comparison with tokamak H-mode power threshold as a function of the position of magnetic axis.

$$P_{\text{Scaling}} = 0.050 \bar{n}_e^{-0.46} B^{0.87} S^{0.84} (2/M)$$

where S and M are the surface area of plasma and mass number of fuel gas, respectively. The threshold in outer shifted configuration is comparable to the scaling while it is 2.5 times larger in inner-shifted one. In the case of limiter H-mode there are no scaling and few reports on the threshold. Twice larger threshold in limiter H-mode has been reported from TEXT-Upgrade [8]. Although it is not certain that this is typical in tokamaks, the threshold in CHS is almost comparable or less than that in tokamaks.

4. Summary

ETB is observed in CHS and the power threshold increases with increasing electron density and magnetic field. It also depends on the magnetic configuration. This implies that there are hidden parameters which relate to the configuration. The ratio of threshold power in CHS to tokamak H-mode scaling is in the range of 1 to 2.5 and depends on the configuration.

References

- [1] K. Toi *et al.*, Plasma Phys. Control. Fusion 38 (1996) 1289.
- [2] S. Okamura *et al.*, J. Plasma Fusion Res. Vol.79, No.10 (2003) 977.
- [3] S. Okamura *et al.*, Plasma Phys. Control. Fusion 46 (2004) A113.
- [4] H. Yamada *et al.*, Proc. of 31th EPS Conf. on Fusion and Plasma Phys. ECA Vol. 28G, (2004) P-5 099.
- [5] K. Hanatani, F-P. Penningfeld, Nucl. Fusion, 32 (1992) 1769
- [6] T. Minami *et al.*, submitted to J. Plasma Fusion Res.
- [7] J.A. Snipes *et al.*, Fusion Energy 2002 (Proc. 19th Int. Conf. Lyon, 2002), CT/P-04
- [8] D.R. Roberts *et al.*, Plasma Phys. Control. Fusion 38 (1996) 1117.